Biointerface Research in Applied Chemistry
Open-Access Journal (ISSN: 2069-5837)

Article
Volume 13, Issue 5, 2023, 456
https://doi.org/10.33263/BRIAC135.456

Juxtaposing the Reactivity Descriptors of Plastic Monomers with their Binding Affinity at the Novel Polyester Hydrolase Target using Conceptual DFT and Machine Learning

Chidi Edbert Duru [1,*], Christian Ebere Enyoh [2], Ijeoma Akunna Duru [3]

[1] Surface Chemistry and Environmental Technology (SCENT) Research Group, Department of Chemistry, Imo State University, Owerri, PMB 2000, Imo State, Nigeria.; chidiedbertduru@gmail.com(C.E.D.);
[2] Graduate School of Science and Engineering, Saitama University, 255 Shimo-Okubo, Sakura-ku, Saitama City, Saitama 338-8570, Japan; cenyoh@gmail.com(C.E.E.);
[3] Federal University of Technology Owerri, Department of Chemistry, PMB 1526, Imo State Nigeria.; iduru015@gmail.com(I.A.D.);
* Correspondence: chidiedbertduru@gmail.com(C.E.D.);

Scopus Author ID26655376900
Received: 12.09.2022; Accepted: 31.10.2022; Published: 24.12.2022

Abstract: The binding of short plastic polymer intermediates or monomers on microbial enzymes is a very important process in polymer degradation and the release of energy for the survival of the microbes. In this study, the molecular docking of six plastic monomers at the novel polyester hydrolase Leipzig 7 (PHL7) active site was performed to determine their selectivity at the enzyme target. The conceptual density functional theory descriptors for the plastic monomers were correlated with their binding affinities at the enzyme target. The most important descriptors for binding of the monomers on the enzyme were predicted from artificial neural networks (ANN) analysis. The results showed that polyethylene terephthalate, polycarbonate, and polyamide, with binding affinities – 5.3 kcal/mol, – 5.3 kcal/mol, and – 4.7 kcal/mol, respectively, were the most stable compounds at the PHL7 target. The binding affinity gave a very good correlation with the binding energy of the monomers while correlating poorly with the total energy, HOMO energy, LUMO energy, energy gap, and electronic chemical potential.ANN analysis predicted that the monomers' binding energy and molecular mass were the most important properties for its binding at the PHL7 target and, by extension, its degradation.

Keywords: polymer degradation; polyester hydrolase Leipzig 7; molecular docking; density functional theory; artificial neural networks.

1. Introduction

Most synthetic polymers used to make plastics are formed from chains of carbon atoms surrounded by other elements such as hydrogen, oxygen, nitrogen, and sulfide [1]. Since their manufacture started in the 1950s, these polymers have been used in every aspect of our lives. Plastic production has increased to keep up with global demand daily. According to reports, the manufacturing of single-use, throw-away plastic materials, which make up around 50 % of all plastic items, is mostly to blame for the rise in plastic production. Due to the tremendous growth in the disposal of plastics, which are largely non-biodegradable and accumulate in the environment, our land and oceans have been contaminated. Only 21 % of plastics generated

worldwide are effectively dealt with; the remainder is dumped on land, where it builds up and pollutes the environment, or in the oceans, where it causes water contamination [2]. These plastics often break down into microplastics and nanoplastics in the environment. Millions of marine creatures, including endangered species, perish each year as a result of microplastics and nanoplastics presence in the oceans. Entanglement and ingestion are two prevalent causes of animal mortality in water and land [3]. When techniques like incineration are employed to eliminate garbage, the accumulation of plastic waste in the environment leads to chemical contamination. In making plastic, chemicals like ethylene, vinyl chloride, terephthalic acid, and bisphenol, most frequently used in consumer-based plastic products, impact negatively on human health, increasing the risk of cancer, endocrine disorders, congenital disabilities, and other illnesses [4].

Since it is impossible to entirely stop manufacturing these incredibly adaptable and widely used plastic items, people are now eager to discover more effective and quicker means of dealing with the huge buildup of this harmful chemical. The solution is undoubtedly within the grasp of researchers, who are continuously trying to develop a biologically safe method to remove plastic trash collecting at an alarming rate [5]. Currently, many studies have reported that natural enzymes can catalyze the hydrolysis of microplastics as an alternative to chemical processes [6,7]. The bacterial strain*Ideonella sakaiensis*201-F6 was recently found to exhibit a rare ability to grow on and degrade polyethylene terephthalate (PET), using it as a major carbon and energy source [8]. The bacteria cells hold fast to the PET surface and emit a PET hydrolase, which converts PET into mono(2-hydroxyethyl)terephthalic acid with trace amounts of terephthalic acid (TPA) and bis(2-hydroxyethyl)-TPA as secondary products. Recently, a novel enzyme, Polyester Hydrolase Leipzig 7 (PHL7), isolated from a compost metagenome, with the ability to completely hydrolyze amorphous PET films, has been reported by Sonnendecker and coworkers [9]. This enzyme releases 91 mg of terephthalic acid per hour and milligrams of the enzyme, the highest so far observed. Structural analysis indicated that the extraordinarily high PET-hydrolyzing activity of PHL7 resulted from the presence of the amino acid leucine at position 210. Substituting this amino acid with another one at this position drastically reduced the PET-hydrolyzing activity of PHL7, clearly indicating that the leucine residue at 210 is responsible for the observed high activity of PHL7.

The release of energy from plastics by microbial enzymatic degradation would involve the hydrolysis of the polymer to the initial monomers used for their formation. The efficient binding of these monomers at the enzyme's active site would therefore determine the ease of energy release. In this study, the molecular docking of some plastic monomers on the active site of the PHL7 enzyme was performed. The binding affinity of these compounds was correlated with their chemical reactivity descriptors using density functional theory (DFT) and artificial neural networks (ANN) to show how these factors affect the binding of the monomers at the enzyme target.

2. Materials and Methods

2.1.Identification and preparation of ligands.

The 3D structure-data files (SDF) of polyvinyl chloride (PVC), polymethyl methacrylate (PMM), polyethylene terephthalate (PET), polyurethane (PU), polyamide (PA), and polycarbonate (PC) were retrieved from the PubChem web server in structure data format (SDF). They were optimized using Open Babel in Python Prescription (version 0.8), which

converted the ligands to the most stable structures using Merk Molecular Force Field 94 (MMFF94).

Table 1. Prepared plastic monomers.

Compound	PubChem CID	Molecular mass (g/mol)	Structure
PET	18721140	222.24	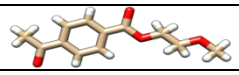
PA	36070	224.30	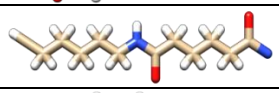
PU	12254	88.11	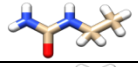
PMM	6658	100.12	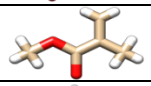
PC	6623	228.29	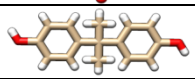
PVC	6338	62.50	

2..2 Preparation of enzyme target and molecular docking studies.

The 3D X-ray crystallographic structure of the novel enzyme Polyester Hydrolase Leipzig 7 (PHL7) with identity 7NEI and resolution 1.30 Å was retrieved from the protein data bank (PDB). Removal of the interfering crystallographic water molecules and minimization of the protein was done using UCSF Chimera 1.14 [10,11]. The enzyme's active site was identified from literature [9] and mapped by the amino acids Phe63, Thr64, Leu93, Ser131, and Leu210. Site-directed docking of the plastic monomers was performed on this target with Autodock Vina in PyRx software version 0.8. The specific site on the receptor was set using the grid box with dimensions: center *x*: – 23.354, center *y*: – 12.204, center *z*: – 8.441, and size *x*: 50.344, size *y*: 49.147, size *z*: 46.109. At the end of the molecular docking, binding poses of the protein-ligand complex were generated, and their scoring results were also created. Hydrogen bonding and other hydrophobic interactions between the enzyme-ligand complex were visualized using Biovia Discovery studio 4.5 [12].

2.3.Density functional theory (DFT) studies.

The optimization of the plastic monomers was performed based on UNIVERSAL force field employing density functional theory (DFT) using DMOL3+ server in Biovia Material Studio 8. The plastic monomers were optimized geometrically to determine quantum parameters such as the energy of the highest occupied molecular orbital (E_{HOMO}), the energy of the lowest unoccupied molecular orbital (E_{LUMO}), energy gap (E_{gap}) (equation 1), and electronic chemical potential (μ) (equation 2). The generalized gradient approximation (GGA) with the Perdew-Burke-Ernzerhof (PBE) was chosen to calculate the geometry optimization [13]. The energy convergence accuracy, maximum force, gradient convergence, displacement convergence, max displacement, and optimal iterations set to 2×10^{-5} Ha, 0.004 Ha/A, 4×10^{-3} Å, 5×10^{-3} A, 0.3 A and 50 respectively. The effect of spin-polarization and pseudopotential was restricted in this paper. The double numerical plus polarization (DNP) was chosen as the basis set, while the semilocal generalized gradient approximation (GGA) and Perdew-Burke-Ernzerhof (PBE) were set as the DFT-Exchange co-relation potential. The self-consistent

(SCF) field tolerance was set to 1×10^{-5} Ha, charge mixing to 0.25 Ha, and the Direct Inversion in the Iterative Subspace (DIIS) size was set to 6 to speed up the convergence of SCF.

$$E_{gap} = E_{LUMO} - E_{HUMO} \quad (1)$$

$$\mu = \frac{E_{HUMO} - E_{LUMO}}{2} \quad (2)$$

Data from the binding affinity and DFT studies were correlated by linear regression using Microsoft Excel 2013.

2.4.Artificial neural network (ANN) analysis.

Computational models with numerous processing layers may learn data representations at various abstraction levels through machine learning. The current study employed a feedforward artificial neural network (ANNs) of many perceptron layers (with threshold activation) for deep learning. A minimum of three layers of nodes make up this ANN: the input layer, the hidden layer, and the output layer. Each node, except the input nodes, is a neuron that employs a nonlinear activation function. Backpropagation is a supervised learning method that the ANN uses during training. The network information for the ANN is summarized in Table 2.

Table 2. Network Information for the ANNs.

Network Information			
Input Layer	Covariates	1	ENERGY
		2	BINDING ENERGY
		3	HOMO
		4	LUMO
		5	ENERGY GAP
		6	ELECTRONIC CHEMICAL POTENTIAL
		7	MOLECULAR MASS
	Number of Units[a]		7
	Rescaling Method for Covariates		Standardized
Hidden Layer(s)	Number of Hidden Layers		1
	Number of Units in Hidden Layer 1[a]		6
	Activation Function		Hyperbolic tangent
Output Layer	Dependent Variables	1	BINDING AFFINITY
	Number of Units		1
	Rescaling Method for Scale Dependents		Standardized
	Activation Function		Identity
	Error Function		Sum of Squares

a. Excluding the bias unit

The input layers include the determined variables from the DFT study: energy, binding energy, molecular mass, HOMO, LUMO, energy gap, and electronic chemical potential. The ANNs used 86 % of the input data to train the model, while 14 % was used for testing the model. The ANN had one hidden layer based on a hyperbolic tangent activation function determined by automatic architecture. In this study's case, the dependent variable, or binary classifications, is contained in the output layer. The output layer's dependent variable (binding affinity on PHL7) and the input layer's independent variables were examined by the ANN during training to see how they specifically relate to one another. The hidden layer's nodes include mathematical functions that define the relationships. Once the connections (mathematical functions) have been established, the testing data were used to validate them. Error functions, such as the relative error (RE) and the sum of squares error (SSE) shown in

equations 1 and 2, were used to verify and evaluate how well the ANN model predicted the output.

$$RE = \left|\frac{BA_A - BA_P}{BA_P}\right| * 100 \quad (1)$$

$$SSE = \sum(BA_P - BA_A)^2 \quad (2)$$

where

$(BA)_P$: is the estimated value of the binding affinity in kcal/mol by the ANN model

$(BA)_A$, is the experimental value of the binding affinity in kcal/mol

3. Results and Discussion

3.1.Molecular docking studies.

The hydrolysis of plastics by enzymatic means is a promising strategy to depolymerize and degrade plastic wastes into monomers for recycling or mineralize them into carbon dioxide and water [14].

Table 3. Binding affinity of plastic monomers at PHL7 active site.

Compound	Protein-ligand complex	Binding affinity (kcal/mol)	Protein-ligand interactions
PET	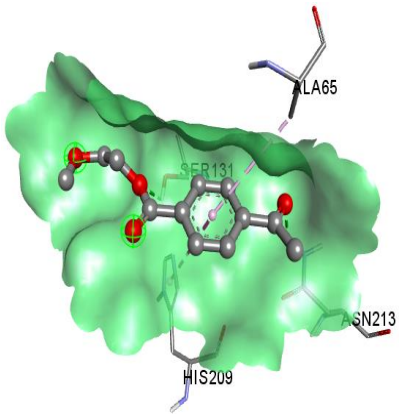	-5.3	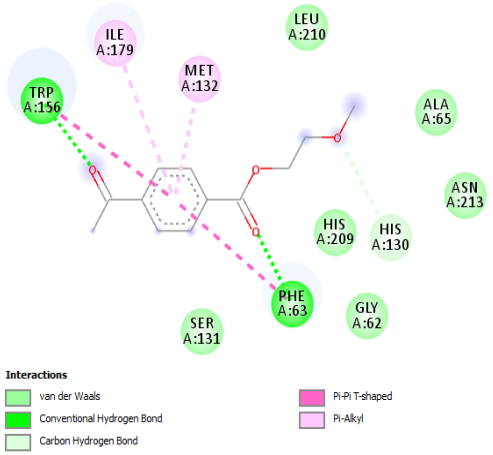
PA	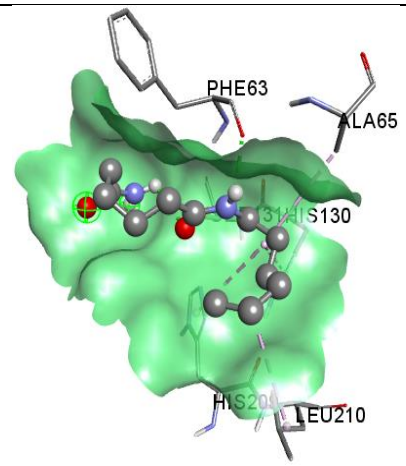	-4.7	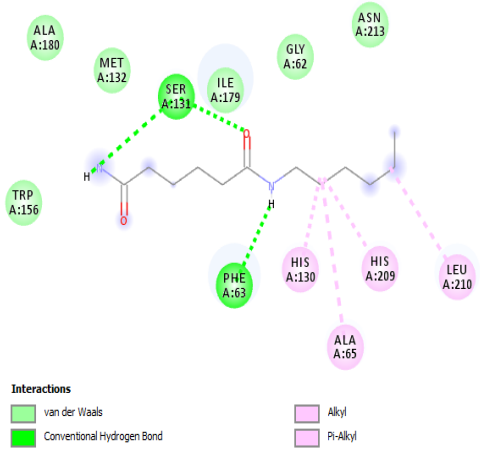

Compound	Protein-ligand complex	Binding affinity (kcal/mol)	Protein-ligand interactions
PU	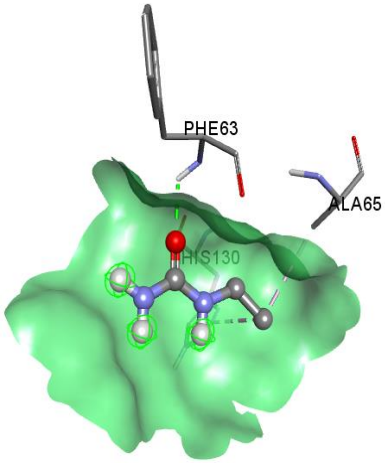	-3.3	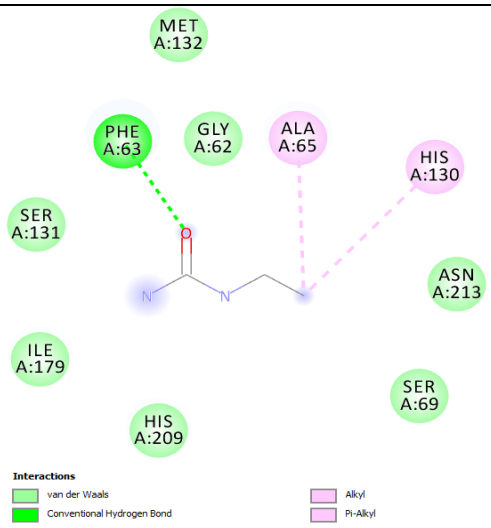
PMM	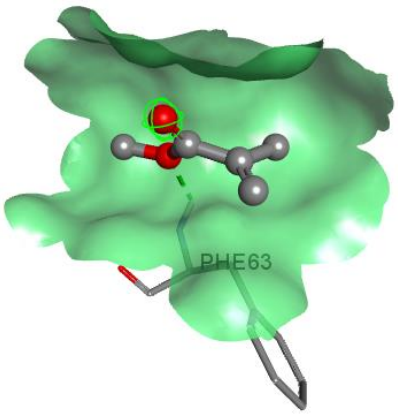	-3.4	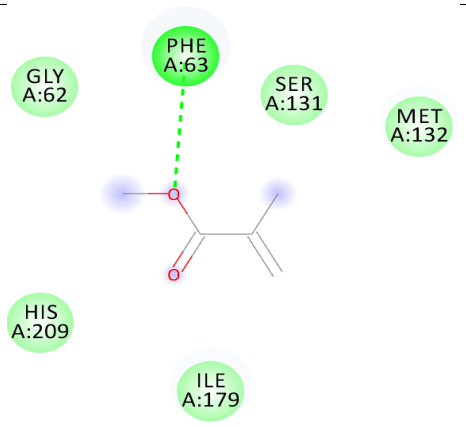
PC	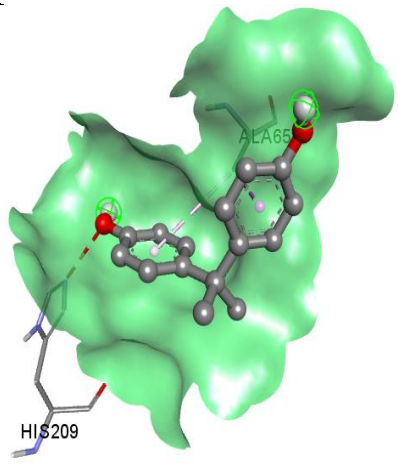	-5.3	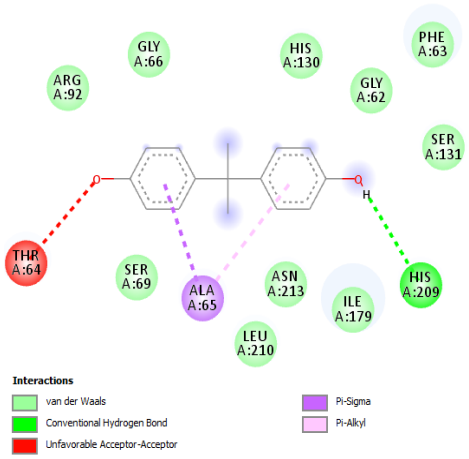

Compound	Protein-ligand complex	Binding affinity (kcal/mol)	Protein-ligand interactions
PVC	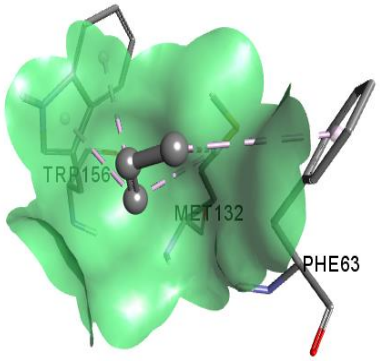	-1.7	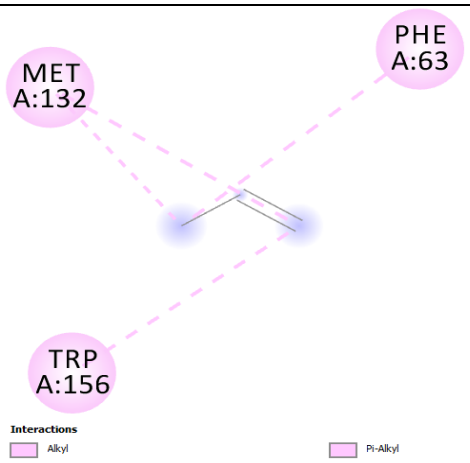

During this process, the microorganism excretions extracellular enzymes, attach the enzyme to the plastic surface and then hydrolyze the plastic to short polymer intermediates or monomer units. These intermediates or monomers are ultimately assimilated by microbial cells as a carbon source to release carbon dioxide. The binding affinities of the plastic monomers at the PHL7 target and their interactions with the amino acids at the active site are shown in Table 3.

The binding affinity of PET (– 5.3 kcal/mol) and PC (– 5.3 kcal/mol) were similar and also the highest, followed by PA (– 4.7 kcal/mol). The binding affinity of PMM, PU, and PVC (– 3.4 kcal/mol, – 3.3 kcal/mol, and – 1.7 kcal/mol, respectively) were low compared to the reference monomer PET. PET and PC molecules contain aromatic rings, and their pi-interactions with the amino acids at the enzyme's active site could be responsible for their better stability at the target. The interactions of the carbonyl, amine and ether functional groups were also important in stabilizing the monomers at the active site. The interaction between the amino acid leucine at position 210 in PET, PC, and PA was nonexistent in all the PMM, PU, and PVC interactions. This amino acid located at the active site of the PHL7 enzyme has been reported to be responsible for its high activity [9]. The inability of PMM, PU, and PVC to interact with leu210 could be a factor responsible for their poor binding at the PHL7 active site.

3.2.DFT studies.

Optimization of the geometry of molecules plays a significant role in the bulk of computational chemistry studies, which concentrate on the structure and reactivity of the molecules. The geometry minimization procedure involves arranging a group of atoms in space so that their positions on the potential energy surface are stationary and their net interatomic forces are as near to zero as is tolerable [15]. Finding the spot where the energy is lowest is the objective of geometry optimization since this is the most stable configuration for the molecule and is most likely to happen in nature. The potential energy and system temperature for the plastic monomers in this study are displayed in Figure 1. It is possible to determine whether or not the model system is in equilibrium using temperature and potential energy equilibrium criteria. For the model system to achieve a balanced state, the temperature and potential energy variations should be minimized to 5 % –10 % [16]. The plastic monomers' potential energy curve and temperature were within acceptable bounds, indicating that the simulation system had reached equilibrium.

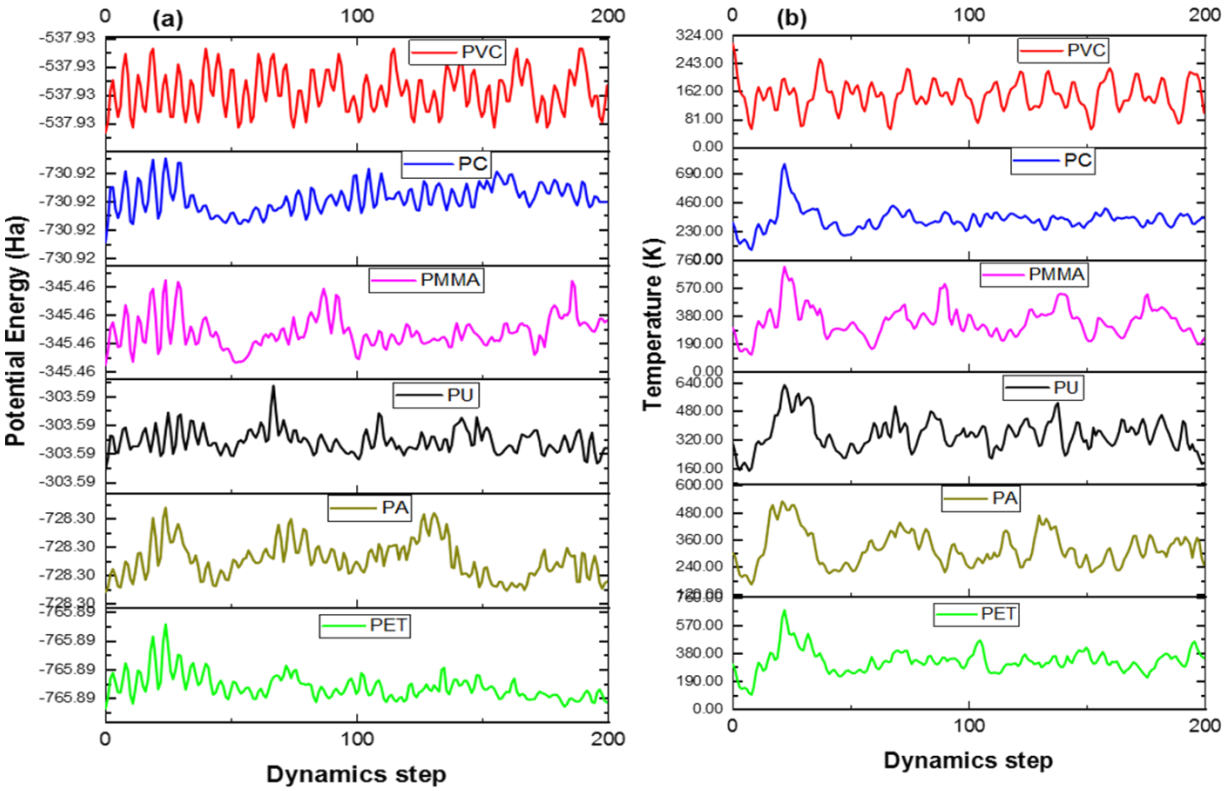

Figure 1. The potential energy and system temperature of the monomers.

The highest occupied molecular orbital (HOMO) and lowest unoccupied molecular orbital (LUMO) diagrams of the plastic monomers are seen in Figure 2.

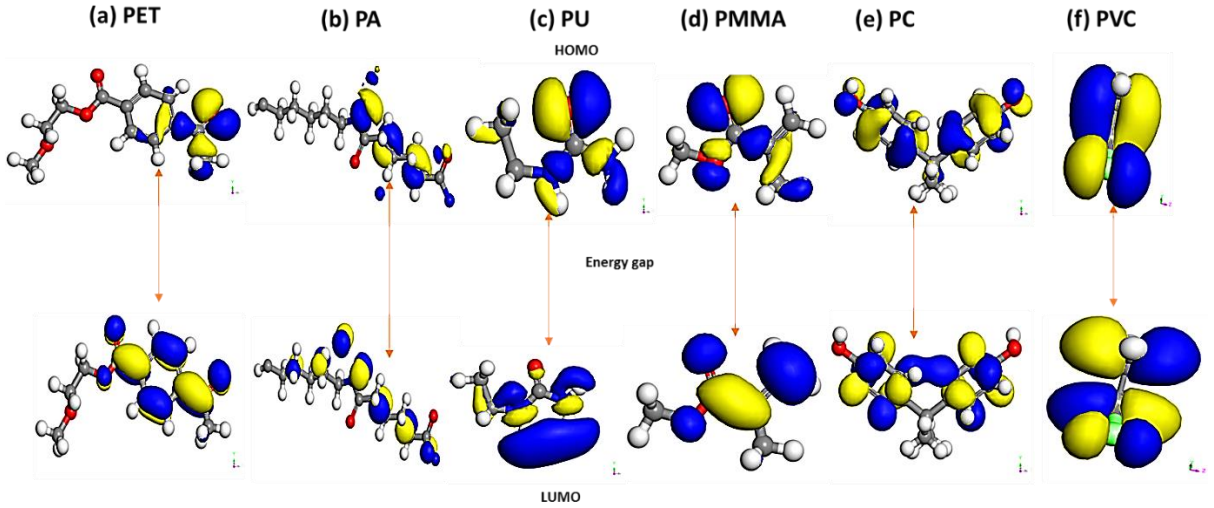

Figure 2. HOMO and LUMO of the monomers.

The reactivity indices, which include total energy, HOMO (E_{HOMO}), LUMO (E_{LUMO}), energy gap (E_{gap}), and electronic chemical potential (μ) are presented in Table 4.

Table 4. Quantum chemical parameters of the different monomers.

Plastics	E_T (Ha)	$E_{binding}$(Ha)	HOMO (eV)	LUMO (eV)	E_{gap} (eV)	μ (eV)
PET	-765.942	-5.469	-0.208	-0.107	0.101	-0.051
PA	-728.341	-5.805	-0.181	-0.123	0.058	-0.029
PU	-303.605	-2.172	-0.198	0.029	0.227	-0.114
PMMA	-345.45	-2.509	-0.226	-0.072	0.154	-0.077
PC	-730.962	-6.121	-0.181	-0.033	0.148	-0.074
PVC	-537.932	-0.884	-0.225	-0.035	0.190	-0.095

The total energy is an indication of the stability of a molecule. The total energy of the monomers ranged from -303.605 Ha for PU to -765.942 Ha for PET. The molecular energy showed a weak correlation (R^2 = 0.4282) with the binding affinity of the molecules (Figure 3a). When it comes to particle removal from a system of particles or particle disassembly, binding energy ($E_{binding}$) is the minimum energy necessary to separate a system into individual components. Negative binding energy means the compound is bound spontaneously at the site (more negative binding energy means more stability). The binding energy of the monomers strongly correlated with their binding affinity at the PHL7 with R^2 = 0.9267 (Figure 3b). This result indicates that the lower the binding energy, the lower the binding affinity at the enzyme target and the higher the rate of degradation of the monomer at the enzyme's active site. For example, PVC's binding energy (-0.884 Ha) and binding affinity (-1.7 kcal/mol) were the highest; thus, its degradation at PHL7 active site would be the poorest.

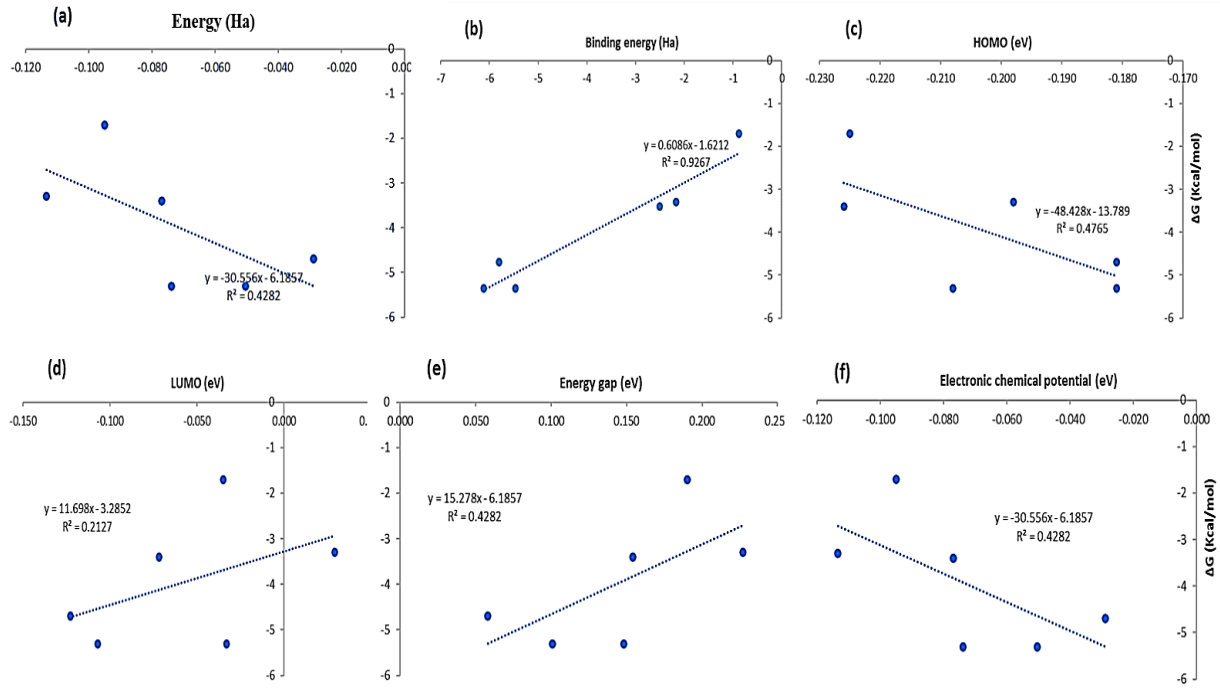

Figure 3. Relationship between binding with **(a)** energy **(b)** binding energy **(c)** HOMO energy **(d)** LUMO **(e)** energy gap **(f)** electronic chemical potential.

The capacity of a molecule to donate electrons is often assessed by its E_{HOMO}, or how efficiently it can transfer electrons to the active site of an enzyme. At the same time, E_{LUMO} often has to do with a molecule's ability to accept electrons, which results in the development of new bonds or interactions [17,18]. The E_{HOMO} and E_{LUMO} values are presented in Table 3 and were correlated with the binding affinities of the monomers at the enzyme target (Figures 3c and 3d). The correlations were generally positive but not significant. E_{HOMO} correlated with R^2 = 0.4765 while E_{LUMO} with R^2 = 0.2127. Rising E_{HOMO} values, therefore, indicate a greater inclination to transfer electron(s) to the appropriate acceptor molecule with low energy and vacant sites. As a result, a high E_{HOMO} correlation promotes binding, enhancing polymer degradation efficiency. The energy difference between the HOMO and LUMO levels is referred to as the energy gap [19]. The energy gap ranged from 0.058 eV in PA to 0.227 eV in PU (Table 3). The correlation with binding affinities of the enzyme showed a weak correlation with R^2 = 0.4282 (Figure 3). Since molecular reactivity is inversely related to the energy gap, the existence of a large energy gap predicts that the molecule will be less predisposed to chemical reactions and reduce its hydrolysis by the PHL7 enzyme. Similarly, the electronic

chemical potential of the monomers showed a weak correlation (R^2 = 0.4282) with the binding affinity (Figure 3f), indicating that it has little effect on the degradation of the monomers at the enzyme target.

3.3.ANN analysis.

A data-driven technique such as ANN was used to obtain an accurate predictive model for the binding affinity of the monomers on the PHL7 enzyme target as a function of their chemical reactivity descriptors. The MLP ANN for the network is presented in Figure 4. One hidden layer makes up the ANN presented here because models with more layers did not fit well. Without hidden layers, ANN operates as a linear regression model that cannot identify nonlinearity, making it impossible for ANN to replicate properly (model) nonlinear patterns in data. The model used in this study has six nodes in the hidden layer.

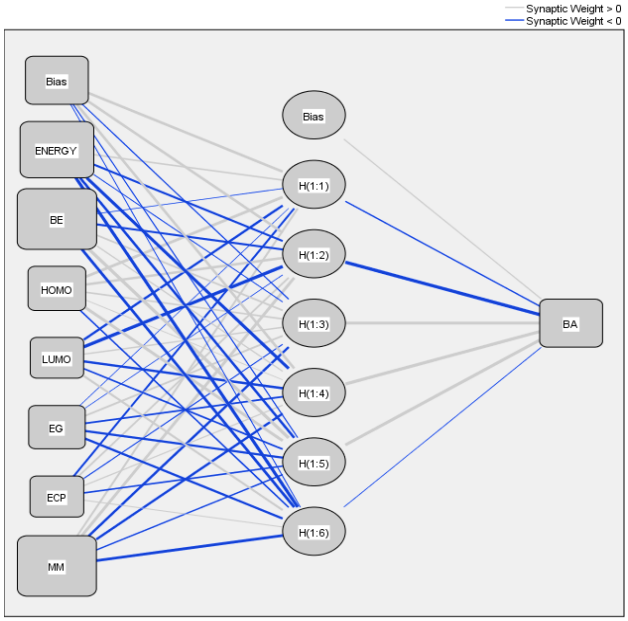

Figure 4. ANNs for predicting plastic monomer degradation based on its reactivity descriptors.

Figure 5 compares the ANN's predicted output values and the binding affinities obtained from molecular docking using linear regression. The ANN predicts the output values as a function of the experimental datasets. The data's regression coefficient of 0.993 demonstrated that the ANNs could accurately predict the binding affinity. The tiny relative error (RE) and a sum of squares error (SSE) between the predicted and actual values were used to confirm this. The RE and SEE were 0.000 and 0.000 during training and testing, respectively.

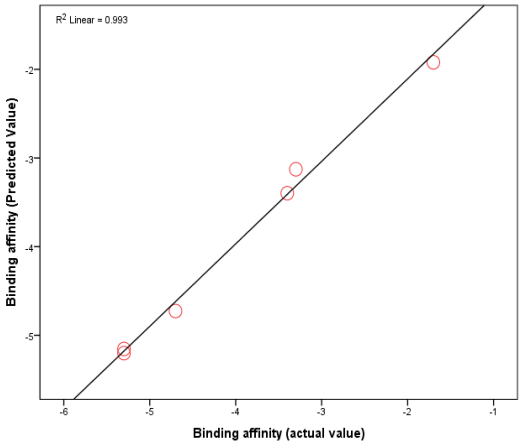

Figure 5. The linear regression of predicted binding affinity from machine learning and actual values.

The ANN analysis determined the most important input variable in predicting the output, and the result is shown in Figure 6.

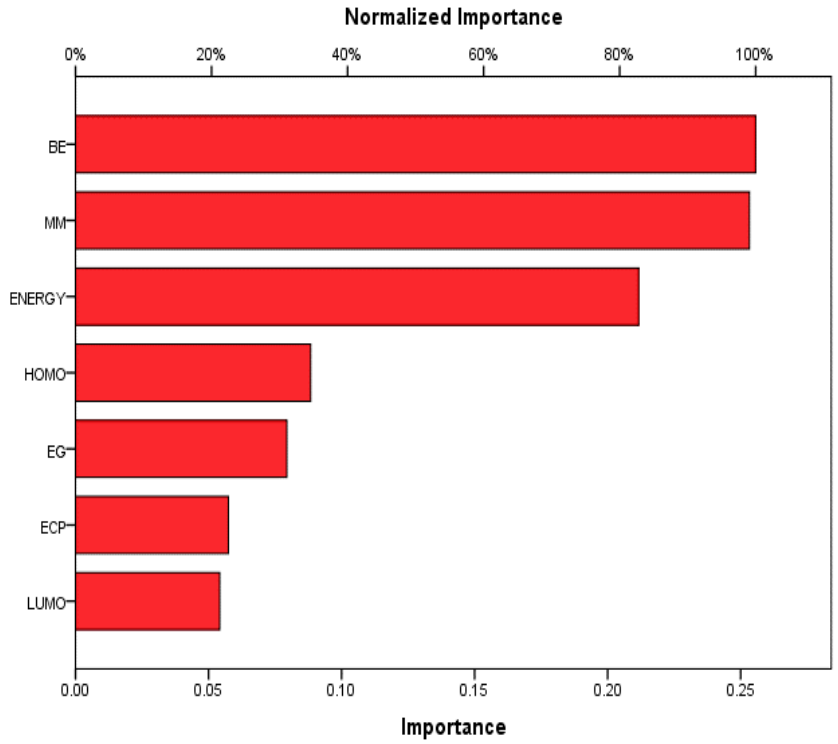

Figure 6. Degree of importance in the enzymatic degradation of the monomers- energy gap (EG), binding energy (BE), electronic chemical potential (ECP), molecular mass (MM).

The binding energy (BE), molecular mass (MM), and energy of the monomer were the most important properties, with normalized importance of 100 %, 99.9 %, and 80 %, respectively. This indicates that these monomer properties mainly determine how much it binds to the HPL7 target and, thus, its degradation. It has been demonstrated in experimental studies that BE, MM, and energy influence the degradation of polymers [20]. It is generally acknowledged that the impact resistance of a material rises with its molecular weight. This is because the polymer can withstand more energy before rupturing since more polymer links must be broken for the polymer to rupture due to a greater degree of entanglement [21]. Therefore, up to a degree, a large molecular weight promotes chemical resistance.

4. Conclusions

The correlation between the binding affinities of plastic monomers at the PHL7 target and their chemical reactivity descriptors from conceptual DFT was studied. Polyvinylchloride, polymethyl methacrylate, polyethylene terephthalate, polyurethane, polyamide, and polycarbonate were shown to have different binding affinity at the polyester hydrolase Leipzig 7 target. The binding affinity of polyethylene terephthalate (– 5.3 kcal/mol), polycarbonate (– 5.3 kcal/mol), and polyamide (– 4.7 kcal/mol) were the best on the enzyme target. The binding affinity of the monomers had a good correlation with their binding energy. In contrast, its correlation with energy, LUMO energy, HOMO energy, energy gap, and electronic chemical potential was poor. Artificial neural networks prognosticated that binding energy and molecular mass of the monomers were the most important factors responsible for the affinity of the monomers at the PHL7 target.

Funding

This research received no external funding.

Acknowledgments

The authors alone were responsible for all the inputs made in the manuscript.

Conflicts of Interest

The authors declare no conflict of interest.

References

1. Kotova, I. B.; Yu. V. T.; Tsavkelova, E. A.; Egorova, M. A.; Bubnov, I. A.; Malakhova, D. V.; Shirinkina, L. I.; Sokolova, T. G.; Bonch-Osmolovskaya, E. A. Microbial degradation of plastics and approaches to make it more efficient. *Microbiology* **2021**, *90*, 671-701, https://doi.org/10.1134/S0026261721060084.
2. Enyoh, C. E.; Ohiagu, F. O.; Verla, A. W.; Wang, Q.; Shafea, L.; Verla, E. N.; Isiuku, B. O.; Chowdhury, T.; Ibe, F. C.; Chowdhury, M. A. H. Plasti-remediation: Advances in the potential use of environmental plastics for pollutant removal. *Environ Technol Innov* **2021**, *23*, 101791, https://doi.org/10.1016/j.eti.2021.101791.
3. Domenech, J.; Marcos, R. Pathways of human exposure to microplastics, and estimation of the total burden. *Curr Opin Food Sci* **2021**, *39*, 144-151, https://doi.org/10.1016/j.cofs.2021.01.004.
4. Udovicki, B.; Andjelkovic, M.; Cirkovic-Velickovic, T.; Rajkovic, A. Microplastics in food: scoping review on health effects, occurrence, and human exposure. *Int J Food Contam* **2022**, *9*, 7, https://doi.org/10.1186/s40550-022-00093-6.
5. Enyoh, C. E.; Maduka, T. O.; Duru, C.E.; Osigwe, S. C.; Ikpa, C. B.; Wang, Q. In sillico binding affinity studies of microbial enzymatic degradation of plastics. *J Hazard Mater Adv* **2022**, *6*, 100076, https://doi.org/10.1016/j.hazadv.2022.100076.
6. Duru, C. E.; Duru, I. A.; Enyoh, C. E. In silico binding affinity analysis of microplastic compounds on PET hydrolase enzyme target of Ideonella sakaiensis. *Bull Natl Res Cent* **2021**, *45*, 104, https://doi.org/10.1186/s42269-021-00563-5.
7. Temporiti, M. E. E.; Nicola, L.; Nielsen, E.; Tosi, S. Fungal enzymes involved in plastics biodegradation. *Microorganisms* **2022**, *10*, 1180, https://doi.org/10.3390/microorganisms10061180.
8. Zhu, B.; Wang, D.; Wei, N. Enzyme discovery and engineering for sustainable plastic recycling. *Trends Biotechnol* **2022**, *40*, 22-37, https://doi.org/10.1016/j.tibtech.2021.02.008.
9. Sonnendecker, C.; Oeser, J.; Richter, P. K.; Hille, P.; Zhao, Z.; Fischer, C.; Lippold, H.; Blázquez-Sánchez, P.; Engelberger, F.; Ramírez-Sarmiento, C. A.; Oeser, T.; Lihanova, Y.; Frank, R.; Jahnke, H. G.; Billig, S.; Abel, B.; Sträter, N.; Matysik, J.; Zimmermann, W. Low carbon footprint recycling of post-consumer PET plastic with a metagenomic polyester hydrolase. *ChemSusChem* **2022**, *15*, e202101062, https://doi.org/10.1002/cssc.202101062.
10. Duru, C. E.; Duru, I. A.; Bilar, A. Computational investigation of sugar fermentation inhibition by bergenin at the pyruvate decarboxylate isoenzyme 1 target of *Scharomyces cervisiae*. *J Med Plants Stud* **2020**, *8*, 21-25, https://doi.org/10.22271/plants.2020.v8.i6a.1225.
11. Duru, I. A.; Duru, C. E. Molecular docking of compounds in the essential oil of *Ocimium gratissimum* leaf against PIM-1 kinase of *Escherichia coli*. *EJ-CHEM* **2020**, *1*, 1-4, https://doi.org/10.24018/ejchem.2020.1.6.26.
12. BIOVIA, Dassault Systemes, San Diego, Discovery studio modeling environment, **2020**.
13. Zhang, M. Y.; Jiang, H. Accurate prediction of band structure of FeS_2: a hard quest of advanced first-principles approaches. *Front Chem* **2021**, *9*, 747972, https://www.frontiersin.org/articles/10.3389/fchem.2021.747972/full.
14. Tamoor, M.; Samak, N. A.; Jia, Y.; Mushtaq, M. U.; Sher, H.; Bibi, M.; Xing, J. Potential use of microbial enzymes for the conversion of plastic waste into value-added products: a viable solution. *Front Microbiol* **2021**, *12*, 777727, https://doi.org/10.3389/fmicb.2021.777727.
15. Ando, T.; Shimizu, N.; Yamamoto, N.; Matsuzawa, N. N.; Maeshima, H.; Kaneko, H. Design of molecules with low hole and electron reorganization energy using DFT calculations and Bayesian optimization. *J Phys Chem A* **2022**, https://doi.org/10.1021/acs.jpca.2c05229.
16. Enyoh, C. E.; Wang, Q.; Weiqian, W.; Tanzin, C.; Mominul, H. R.; Islam, M. R.; Guo, Y.; Lin, Y.; Kai, X. Sorption of per- and polyfluoroalkyl substances (PFAS) using polyethylene (pe) microplastics as adsorbent:

grand canonical monte carlo and molecular dynamics (GCMC-MD) studies. *Int J Environ Anal Chem* **2022**, https://doi.org/10.1080/03067319.2022.2070016.
17. Singh, J. S.; Khan, M. S.; Uddin, S. A DFT study of vibrational spectra of 5-chlorouracil with molecular structure, HOMO–LUMO, MEPs/ESPs and thermodynamic properties. *Polym Bull* **2022**, https://doi.org/10.1007/s00289-022-04181-7.
18. Duru, C. E.; Duru, I. A. Computational investigation of infrared vibrational frequency shift modes in Schiff base-transition metal complexes. *JAOC* **2022**, *2*, 54-65, https://doi.org/10.22034/JAOC.2022.319433.1041.
19. Duru, I. A.; Duru, C. E. Molecular modeling and density functional theory calculation of the coordination behaviour of 4,5-dichloroimidazole with Cu(II) ion. *Sci Afr* **2020**,*9*, e00533, https://doi.org/10.1016/j.sciaf.2020.e00533.
20. Mamun, A.; Rahman, S. M. M.; Roland, S.; Mahmood, R. Impact of molecular weight on the thermal stability and the miscibility of poly(ε-caprolactone)/polystyrene binary blends. *J Polym Environ* **2018**, *26*, 3511–3519, https://doi.org/10.1007/s10924-018-1236-1.
21. AMCOPOLYMERS. Molecular Weight and the effects on polymer properties. Available online: https://www.amcopolymers.com/resources/blog/molecular-weight-and-its-effects-on-polymer-properties#:~:text=A%20High%20molecular%20weight%20increases%20the%20impact%20resistance%20of%20the,chemical%20resistance%20%2D%20to%20a%20point.